Unified Outage Probability Analysis for Dual-Hop Decode-and-Forward Relaying with Energy Harvesting over $\alpha - \eta - \mu$ Fading Channels

Mohammed S. Aloqlah, *Member, IEEE*, and Abdullah S. Aloqlah, *Student member, IEEE*

***Abstract*—In this paper, we investigate dual-hop decode-and-forward (DF) relaying systems, where the relay node employs energy harvesting from the source's transmitted signal. The study focuses on evaluating the performance of three energy-harvesting (EH) protocols-namely, Ideal Relaying Receiver (IRR), Power-Splitting Relaying (PSR), and Time-Switching Relaying (TSR)- in a non-homogeneous environment. We derive a novel, exact, and unified closed-form expression for the outage probability (OP) of these protocols under independent but non-identically distributed (i.n.i.d.) $\alpha-\eta-\mu$ fading channels. The results demonstrate that increasing the fading parameters improves system performance. The analytical findings are corroborated through extensive numerical evaluations and Monte Carlo simulations, confirming the accuracy of the proposed model.**

***Index Terms*—Outage probability, $\alpha - \eta - \mu$ fading, decode-and-forward, and energy harvesting**

I. Introduction

Low-power wireless techniques, which are heavily deployed in such technologies like the Internet of Things (IoT) and Wireless Sensor Networks (WSNs), have become more numerous due to their capability for widespread communication demands [1]. However, the dependency on battery-powered devices has challenged their usefulness. Energy harvesting (EH) is a promising geration technique, which allows devices to convert environmental energy into electricity, commonly from solar, thermal, wind and radio frequency (RF) sources. Notably, RF energy harvesting is important because it carries both energy and data, thus making it useful for remote applications. This seminal technology has spurred low-cost simultaneous wireless information and power transfer (SWIPT) architecture, which realizes higher spectral efficiency by self-sustaining power and data transmission.

Recent studies on SWIPT-based relay networks have investigated cases where relay nodes can harvest energy from incoming RF signals to perform information forwarding. For example, dual-hop relay design in the Rayleigh fading regime of amplify-and-forward (AF) systems was considered in [2] which compared EH schemes (e.g., IRR, PSR, and TSR). Other analysis studies focused on OP of DF relay networks in underlay cognitive networks leveraging PSR and TSR protocols in Rayleigh fading scenarios [3]. Throughput and ergodic capacity (EC) of DF relaying systems with PSR and TSR protocols were investigated and analytical models were developed in [4]. Other studies including Rabie et al. [5] and Nauryzbayev et al. [6] have carried out researches on OP performance in AF and DF networks with half-duplex (HD) and full-duplex (FD) modes, and performance evaluation in terms of energy efficiency and physical layer security were studied in [7] within wireless power transfer (WPT)-enabled FD-DF networks. Moreover, secrecy rates have been investigated in massive MIMO systems [8], [9] as well as inter-relay interference problems in WPT-MIMO FD schemes [10]. More recent studies, like Ye et al. [11], Xu et al. [12], and Han et al. [13] NOMA integrated with SWIPT network Those works studied symbol error probability (OP) and data rate performance in PS-based cooperative non-orthogonal multiple access (NOMA) setups, and energy efficiency in amplify-and-forward (AF)-NOMA systems operating over Nakagami-m fading channels.

The α-η-μ fading distribution, which extends the widely studied α-μ and η-μ models, offers a comprehensive framework that includes well-known fading distributions (e.g., Rayleigh, Nakagami-m, and Weibull) as special cases. This distribution effectively captures non-linear and non-homogeneous fading behaviors, particularly in scenarios without a line-of-sight (LOS) component. Although prior studies have analyzed the performance of communication systems under α-η-μ fading conditions [14], the integration of EH within these models remains largely unexplored. To the best of the authors' knowledge, no existing research provides a unified analytical framework for SWIPT systems over α-η-μ fading channels, highlighting the novelty of this work.

The remainder of the paper is structured as follows: Section II outlines the system and channel models employed in this study. Section III derives closed-form analytical expressions for the OP of the TSR, PSR, and IRR protocols over i.n.i.d. α-η-μ fading channels. Section IV presents the analytical results alongside Monte Carlo simulations to validate the proposed models. Section V concludes the paper with a summary of the key findings.

II. Channel Model and Energy Harvesting Protocols

A. Channel Model

In this paper, the α-η-μ fading model is employed to represent small-scale signal variations. This generalized model captures a range of commonly encountered fading behaviors, including Rayleigh, Nakagami-m, Hoyt, one-sided Gaussian, Weibull, and η-μ fading, as special cases. The model is particularly useful for characterizing non-linear, non-homogeneous channels, especially in scenarios without LOS components.

The channel gains for the source-relay (S-R) and relay-destination (R-D) links are denoted by ρ_1 and ρ_2, respectively, with the distances between the nodes represented as d_1 and d_2. These channels are modeled as block fading, meaning the fading coefficients remain constant during each block of duration T but vary independently between blocks. The instantaneous signal-to-noise ratio (SNR) for each link, denoted by $W_i = |\rho_i|^2$, for

Mohammed S. Aloqlah is with the Telecommunication Engineering Department, Yarmouk Unioversity, Irbid 21163, Jordan. e-mail: mohamads@yu.edu.jo. Abdullah S. Aloqlah is with Electrical and Computer Engineering Department, Wayne State University, Detroit, MI 48202, USA. e-mail: c_aaloql@wayne.edu}

979-8-3315-2096-0/25/$31.00 ©2025 IEEE

$i \in \{1, 2\}$, follows the $\alpha - \eta - \mu$ distribution, and the probability density function (PDF) of the SNR is given by:

$$f_{W_i}(w) = \frac{\sqrt{\pi}\alpha_i \mu_i^{\mu_i+0.5} h_i^{\mu_i} w^{\frac{\alpha_i}{2}(\mu_i+0.5)-1}}{\Gamma(\mu_i) H_i^{\mu_i-0.5} \Omega_i^{\frac{\alpha_i}{2}(\mu_i+0.5)}} \times \exp\left(-2\mu_i h \left(\frac{w}{\Omega_i}\right)^{\frac{\alpha_i}{2}}\right) I_{\mu_i-\frac{1}{2}}\left(2\mu_i H_i \left(\frac{w}{\Omega_i}\right)^{\frac{\alpha_i}{2}}\right), \tag{1}$$

where i refers to either the S-R or the R-D link, Ω_i denotes the average SNR, $\Gamma(\cdot)$ is the Gamma function, and $I_z(\cdot)$ represents the modified Bessel function of the first kind, as defined in [15, Eq. (9.6.20)]. The parameters α_i, η_i, and μ_i correspond to the non-linearity parameter, the ratio between the in-phase and quadrature scattered wave components, and the number of multipath clusters, respectively. The parameters h_i and H_i depend on the specific signal propagation format as:

$$h_i = \frac{1+\eta_i^2}{4\eta_i}, \quad H_i = \frac{1-\eta_i^2}{4\eta_i}, \quad 0 < \eta_i < 1, \tag{2}$$

for Format I, and

$$h_i = \frac{1}{1-\eta_i^2}, \quad H_i = \frac{\eta_i}{1-\eta_i^2}, \quad -1 < \eta_i < 1, \tag{3}$$

for Format II, where η_i represents the ratio of scattered wave power or the correlation coefficient between the in-phase and quadrature components within each multipath cluster.

Utilizing the identity provided in [16, Eq. (8.445)] and applying a series of algebraic transformations, the PDF of W_i can be written as:

$$f_{W_i}(w) = \frac{\sqrt{\pi}\alpha_i \mu_i^{2\mu_i} h_i^{\mu_i}}{\Gamma(\mu_i)\Omega_i^{\alpha_i\mu_i}} w^{\alpha_i\mu_i-1} \exp\left(-2\mu_i h_i \left(\frac{w}{\Omega_i}\right)^{\frac{\alpha_i}{2}}\right) \times \sum_{k=0}^{\infty} \frac{1}{k!\Gamma(\mu_i+k+0.5)} \left(\mu_i H_i \left(\frac{w}{\Omega_i}\right)^{\frac{\alpha_i}{2}}\right)^{2k}. \tag{4}$$

B. Energy Harvesting in Dual-Hop Relaying Systems

The system under consideration consists of a single-antenna source node, an energy-constrained relay node, and a destination node. Since there is no direct communication path between the source and destination, the data is transmitted through the relay in two sequential phases. The relay, operating without an external power source, relies solely on the energy harvested from the source's signal. The energy consumption for the relay's internal circuitry is assumed to be negligible.

In dual-hop DF relaying systems, communication occurs in two sequential phases. During the first phase, the source node S transmits information to the relay node R using transmission power P_s. In the second phase, the relay node decodes the received information and forwards it to the destination node D. Additionally, the relay node performs EH by extracting energy from the transmitted power during the first phase. Three primary EH protocols have been discussed in the literature: TSR, PSR, and IRR protocols. The operation of these protocols is summarized in the following subsections. Due to space constraints, detailed mathematical modeling of the received signals at nodes R and D is omitted, and interested readers are referred to [2], [5], [17].

1) Time-Switching Relaying Protocol: In TSR, the total transmission time T is divided into three distinct phases: EH, transmission from the source to the relay (S-R), and transmission from the relay to the destination (R-D). These phases are allocated durations ηT, $(1-\eta)T/2$, and $(1-\eta)T/2$, respectively, where η (with $0 \le \eta \le 1$) denotes the EH time factor. This protocol allows the relay to harvest energy initially before transmitting information.

2) Power-Splitting Relaying Protocol: In PSR, the transmission time T is divided into two phases of equal duration. During the first phase, the relay node R splits the received signal's power, using a fraction $(1-\beta)P_s$ for information decoding and allocating the remaining fraction βP_s for energy harvesting. Here, β (where $0 \le \beta \le 1$) represents the power-splitting factor, controlling the trade-off between EH and information decoding.

3) Ideal Relaying Receiver Protocol: The IRR protocol operates similarly to PSR, with the total time T split equally into two phases. However, during the first phase, the entire received signal is utilized for both energy harvesting and information decoding simultaneously, assuming ideal conditions for energy extraction and decoding.

III. Outage Probability Analysis of Relaying Protocols

This section presents a unified framework for evaluating the OP of the aforementioned relaying protocols. The instantaneous end-to-end signal-to-noise ratio (SNR), $\gamma_{\text{eff}}^{\text{DF}}$, for the dual-hop DF relaying system is given by:

$$\gamma_{\text{eff}}^{\text{DF}} = \min(\gamma_1, \gamma_2). \tag{5}$$

Using the expressions from [2] and [5], the individual SNRs γ_1 and γ_2 can be expressed as:

$$\gamma_1 = \phi W_1, \quad \gamma_2 = \varphi W_1 W_2, \tag{6}$$

where ϕ and φ are parameters specific to each protocol. For the TSR and IRR protocols, $\phi = \frac{P_s}{d_1^{\zeta_1}\sigma_1^2}$, while for the PSR protocol, $\phi = \frac{(1-\beta)P_s}{d_1^{\zeta_1}\sigma_1^2}$. Similarly, the parameter φ is given by [17]:

$$\varphi = \begin{cases} \frac{2\varepsilon\eta P_s}{(1-\eta)d_1^{\zeta_1} d_2^{\zeta_2}\sigma_2^2}, & \text{(TSR)} \\ \frac{\varepsilon\beta P_s}{d_1^{\zeta_1} d_2^{\zeta_2}\sigma_2^2}, & \text{(PSR)} \\ \frac{\varepsilon P_s}{d_1^{\zeta_1} d_2^{\zeta_2}\sigma_2^2}, & \text{(IRR)} \end{cases} \tag{7}$$

where ε (with $0 < \varepsilon < 1$) denotes the energy conversion efficiency, which depends on the rectification process and energy harvesting circuitry.

The OP, which measures the probability of the end-to-end SNR falling below a specified threshold γ_{th}, is expressed as:

$$\begin{aligned} \text{OP} &= \Pr\{\gamma_{\text{eff}}^{\text{DF}} < \gamma_{\text{th}}\} \\ &= 1 - \Pr\{\gamma_1 > \gamma_{\text{th}}, \gamma_2 > \gamma_{\text{th}}\} \\ &= 1 - \Pr\left[W_1 > \frac{\gamma_{\text{th}}}{\phi}, W_1 W_2 > \frac{\gamma_{\text{th}}}{\varphi}\right]. \end{aligned} \tag{8}$$

For the TSR protocol, $\gamma_{\text{th}} = 2^{2R/(1-\eta)} - 1$, while for the PSR and IRR protocols, $\gamma_{\text{th}} = 2^{2R} - 1$, where R represents the target data rate.

The OP can be further expressed as:

$$\text{OP} = 1 - \int_{\gamma_{\text{th}}/\phi}^{\infty} \bar{F}_{W_2}\left(\frac{\gamma_{\text{th}}}{\varphi w}\right) f_{W_1}(w)\, dw, \tag{9}$$

where $f_{W_1}(\cdot)$ and $\bar{F}_{W_2}(\cdot)$ denote the PDF and the complementary cumulative distribution function (CCDF) of the $\alpha-\eta-\mu$ fading channels, respectively. We insert (4) into $\bar{F}_{W_2}(W) = \int_W^\infty f_{W2}(z)dz$ and applying [16, Eq. (3.381.8)], the CCDF of W_2 is given by:

$$\bar{F}_{W_2}(w) = \frac{\sqrt{\pi}}{\Gamma(\mu_2)\, 2^{2\mu_2-1}\, h_2^{\mu_2}} \sum_{k=0}^{\infty} \frac{1}{k!\Gamma(\mu_2+k+0.5)} \left(\frac{H_2}{2\, h_2}\right)^{2k} \times \Gamma\left(2(\mu_2+k), 2\mu_2\, h_2 \left(\frac{w}{\Omega_2}\right)^{\frac{\alpha_2}{2}}\right), \tag{10}$$

where $\Gamma(\cdot,\cdot)$ is the upper incomplete gamma function as given in [16, Eq. (8.350.2)].

Substituting (4) and (10) into (9), we express the OP as

$$\begin{aligned} \text{OP} =& 1 - \frac{\pi\alpha_1 \mu_1^{2\mu_1} h_1^{\mu_1}}{\Gamma(\mu_1)\bar{\gamma}_1^{\alpha_1\mu_1}\Gamma(\mu_2)\, 2^{2\mu_2-1}\, h_2^{\mu_2}} \\ &\times \sum_{k=0}^{\infty} \frac{1}{k!\Gamma(\mu_1+k+0.5)} \left(\frac{\mu_1 H_1}{\Omega_1{}^{\frac{\alpha_1}{2}}}\right)^{2k} \\ &\times \sum_{l=0}^{\infty} \frac{1}{l!\Gamma(\mu_2+l+0.5)} \left(\frac{H_2}{2\, h_2}\right)^{2l} \\ &\times \int_{\gamma_{\text{th}}/\phi}^{\infty} w^{\alpha_1(\mu_1+k)-1} \exp\left(-2\mu_1 h_1 \left(\frac{w}{\Omega_1}\right)^{\frac{\alpha_1}{2}}\right) \\ &\times \Gamma\left(2(\mu_2+l), 2\mu_2\, h_2 \left(\frac{\gamma_{\text{th}}}{\varphi w \Omega_2}\right)^{\frac{\alpha_2}{2}}\right) dw. \end{aligned} \tag{11}$$

Accordingly, the OP can be reformulated as

$$\begin{aligned} \text{OP} =& 1 - \frac{\pi\alpha_1 \mu_1^{2\mu_1} h_1^{\mu_1}}{\Gamma(\mu_1)\Omega_1{}^{\alpha_1\mu_1}\Gamma(\mu_2)\, 2^{2\mu_2-1}\, h_2^{\mu_2}} \\ &\times \sum_{k=0}^{\infty}\sum_{l=0}^{\infty} \frac{1}{k!\Gamma(\mu_1+k+0.5)} \left(\frac{\mu_1 H_1}{\Omega_1{}^{\frac{\alpha_1}{2}}}\right)^{2k} \\ &\times \frac{1}{l!\Gamma(\mu_2+l+0.5)} \left(\frac{H_2}{2\, h_2}\right)^{2l} \mathcal{I}_1, \end{aligned} \tag{12}$$

where

$$\begin{aligned} \mathcal{I}_1 =& \int_{\gamma_{\text{th}}/\phi}^{\infty} w^{\alpha_1(\mu_1+k)-1} \exp\left(-2\mu_1 h_1 \left(\frac{w}{\Omega_1}\right)^{\frac{\alpha_1}{2}}\right) \\ &\times \Gamma\left(2(\mu_2+l), 2\mu_2\, h_2 \left(\frac{\gamma_{\text{th}}}{\varphi w \Omega_2}\right)^{\frac{\alpha_2}{2}}\right) dw, \end{aligned} \tag{13}$$

The latter integral in (13), evaluated with respect to w, can be efficiently computed by applying a series expansion to the upper incomplete gamma function [9, Eq. (8.352.2)] when μ_2 is half integer. After performing further mathematical manipulations (13) can be written as

$$\mathcal{I}_1 = \sum_{m=0}^{2(\mu_2+l)-1} \frac{(2(\mu_2+l)-1)!}{m!} \left(2\mu_2\, h_2 \left(\frac{\gamma_{\text{th}}}{\varphi\Omega_2}\right)^{\frac{\alpha_2}{2}}\right)^m \mathcal{I}_2, \tag{14}$$

where

$$\begin{aligned} \mathcal{I}_2 =& \int_{\gamma_{\text{th}}/\phi}^{\infty} w^{\alpha_1(\mu_1+k)-\frac{\alpha_2}{2}m-1} \exp\left(-2\mu_1 h_1 \left(\frac{w}{\Omega_1}\right)^{\frac{\alpha_1}{2}}\right) \\ &\times \exp\left(-2\mu_2\, h_2 \left(\frac{\gamma_{\text{th}}}{\varphi w \Omega_2}\right)^{\frac{\alpha_2}{2}}\right) dw. \end{aligned} \tag{15}$$

The closed-form solution for the integral in (15) can be derived by employing the methodology outlined in [18]. The result is presented in (16) at the bottom of the next page, expressed in terms of the Fox's H-function, $H_{p,q}^{m,n}[\cdot]$.

Finally, utilizing the results from (16), (14), and (12) along with further algebraic manipulations, we derive a closed-form expression for the OP of the energy-harvesting dual-hop DF system for various relaying protocols. This final expression, shown in (17), provides a critical performance metric related to the system's grade of service.

IV. Numerical Results

This section presents the performance results for the OP of the considered dual-hop relaying system. The analytical outcomes are validated through Monte Carlo simulations. Unless specified otherwise, the source-destination separation is fixed at 40 meters, with the parameters $\Omega_1 = \frac{1}{3}$, $\Omega_2 = \frac{2}{3}$, $R = 0.5$, $\varepsilon = 0.75$, and $\sigma_1^2 = \sigma_2^2 = 1$.

Fig. 1 depicts the variation of OP with respect to the source transmission power P_s for the TSR protocol, considering $\eta_1 = 0.5$. In this scenario, the relay is positioned equidistant from both the source and destination nodes, i.e., $d_1 = 20\,\text{m}$. The results show a decrease in OP as the parameters α_1 and/or μ_1 increase. This behavior arises from the fact that α_1 reflects the power-law exponent of the received signal, while μ_1 corresponds to the number of multipath components within each scattering cluster. Similar trends are observed for the PSR and Ideal Relaying IRR protocols; however, these results are omitted due to space constraints.

Fig. 2 illustrates the variation in OP with respect to the P_s for the TSR protocol, with α = 1.5. In this setup, the relay is located equidistant from both the source and destination nodes. The results indicate a reduction in OP as the parameters η_1 and/or μ_1 increase. This trend occurs because η_1 represents the ratio between the in-phase and quadrature components of scattered waves, while μ_1 reflects the number of multipath components in each scattering cluster.

Fig. 3 demonstrates the relationship between OP and the parameters η and β for both the TSR and PSR protocols. The figure indicates that as η and β increase, system performance improves. However, when either parameter approaches its boundary values (i.e., 0 or 1), a significant degradation in OP is observed. This degradation occurs because, at $\beta = 1$, no energy remains for information decoding, and at $\eta = 1$, the entire time frame is allocated to energy harvesting, leaving no time for S-R transmission. Thus, although increasing η and β can enhance performance under certain conditions, it may also negatively affect the system. Moreover, the results illustrate that higher values of α_2 and/or μ_2 further improve OP performance, affirming the impact of these parameters.

Fig. 4 examines the effect of the source-relay distance (d_1) and the path-loss exponents ζ_1 and ζ_2 on OP performance for symmetrical channels with $\alpha_1 = \alpha_2 = 3$, $\eta_1 = \eta_2 = 2$ and $\mu_1 = \mu_2 = 2$. In both scenarios — whether $\zeta_1 > \zeta_2$ or $\zeta_2 > \zeta_1$—OP initially worsens as d_1 increases. However, beyond a certain distance threshold (d_0), the OP starts to improve with increasing d_1. Additionally, the results indicate that, when $\zeta_1 > \zeta_2$, the system performs better compared to the reverse case ($\zeta_2 > \zeta_1$). However, when the relay is positioned midway between the source and destination nodes (i.e., $d_1 = 20\,\text{m}$), this behavior is

reversed. This suggests that, when the S-R link exhibits superior channel conditions compared to the R-D link, the optimal relay placement should be closer to the source. Conversely, when the R-D link is more favorable, the relay should be placed nearer to the destination.

V. Conclusion

This paper demonstrates a detailed performance evaluation of dual-hop DF relaying systems with EH features, emphasizing on three fundamental protocols: IRR, PSR, and TSR. A unified, precise formula for the OP was derived under i.n.i.d. α-η-μ channel fading models, delivering a resilient framework for analyzing these EH strategies in non-homogeneous conditions. The analytical results demonstrate that system performance enhances with increasing fading factors, underlining the importance of link quality in enhancing the robustness of EH-enabled relaying systems. The accuracy of the proposed model is further Corroborated through Comprehensive numerical analyses and Monte Carlo simulations, illustrating close agreement between theoretical predictions and empirical results. These findings underscore the practicality of IRR, PSR, and TSR protocols in future wireless networks, especially under realistic fading conditions and more complex wireless environments.

References

[1] X. Lu, P. Wang, D. Niyato, D. I. Kim, and Z. Han, "Wireless networks with rf energy harvesting: A contemporary survey," *IEEE Communications Surveys & Tutorials*, vol. 17, no. 2, pp. 757–789, 2014.

[2] A. A. Nasir, X. Zhou, S. Durrani, and R. A. Kennedy, "Relaying protocols for wireless energy harvesting and information processing," *IEEE Transactions on Wireless Communications*, vol. 12, no. 7, pp. 3622–3636, 2013.

[3] S. Arzykulov, G. Nauryzbayev, T. A. Tsiftsis, and M. Abdallah, "On the performance of wireless powered cognitive relay network with interference alignment," *IEEE Transactions on Communications*, vol. 66, no. 9, pp. 3825–3836, 2018.

[4] A. A. Nasir, X. Zhou, S. Durrani, and R. A. Kennedy, "Throughput and ergodic capacity of wireless energy harvesting based df relaying network," in *2014 IEEE international conference on communications (ICC)*. IEEE, 2014, pp. 4066–4071.

[5] K. M. Rabie, B. Adebisi, and M.-S. Alouini, "Wireless power transfer in cooperative df relaying networks with log-normal fading," in *2016 IEEE Global Communications Conference (GLOBECOM)*. IEEE, 2016, pp. 1–6.

[6] G. Nauryzbayev, M. Abdallah, and K. Rabie, "Outage probability of full-duplex af and df relaying systems over α-μ channels," in *IEEE Vehicular Technology Conference (IEEE VTC2018-Fall)*, 2018, pp. 1–6.

[7] Z. Chang, X. Hou, X. Guo, T. Ristaniemi, and Z. Han, "Secure and energy-efficient resource allocation for wireless power enabled full-/half-duplex multiple-antenna relay systems," *IEEE Transactions on Vehicular Technology*, vol. 66, no. 12, pp. 11 208–11 219, 2017.

[8] J. Zhu, Y. Li, N. Wang, and W. Xu, "Wireless information and power transfer in secure massive mimo downlink with phase noise," *IEEE Wireless Communications Letters*, vol. 6, no. 3, pp. 298–301, 2017.

[9] Z. Chang, Z. Wang, X. Guo, Z. Han, and T. Ristaniemi, "Energy efficient resource allocation for wireless power transfer enabled massive mimo system,"

$$
\begin{aligned}
\mathcal{J}_2 =& \frac{4}{\alpha_1\alpha_2}\frac{1}{\left(\frac{2\mu_1 h_1}{\Omega_1{}^{\frac{\alpha_1}{2}}}\right)^{\frac{2}{\alpha_1}\left(\alpha_1(\mu_1+k)-\frac{\alpha_2}{2}m\right)}}\mathrm{H}_{0,2}^{2,0}\left[\frac{\left(\frac{2\mu_1 h_1}{\Omega_1{}^{\frac{\alpha_1}{2}}}\right)^{\frac{2}{\alpha_1}}\left(2\mu_2\, h_2\left(\frac{\gamma_{\text{th}}}{\varphi\Omega_2}\right)^{\frac{\alpha_2}{2}}\right)^{\frac{2}{\alpha_2}}}{\varphi}\gamma_{\text{th}}\,\middle|\,\begin{matrix}---\\ \left(0,\frac{2}{\alpha_2}\right),\left(\frac{2}{\alpha_1}\left(\alpha_1(\mu_1+k)-\frac{\alpha_2}{2}m\right),\frac{2}{\alpha_1}\right)\end{matrix}\right]\\
&-\frac{4}{\alpha_1\alpha_2}\frac{\Gamma\left(1+\frac{1}{1-\delta}\right)}{\left(\frac{2\mu_1 h_1}{\Omega_1{}^{\frac{\alpha_1}{2}}}(1-\delta)\right)^{\frac{2}{\alpha_1}\left(\alpha_1(\mu_1+k)-\frac{\alpha_2}{2}m\right)}}\mathrm{H}_{0,2}^{2,0}\left[\frac{\left(\frac{2\mu_1 h_1}{\Omega_1{}^{\frac{\alpha_1}{2}}}(1-\delta)\right)^{\frac{2}{\alpha_1}}\left(2\mu_2\, h_2\left(\frac{\gamma_{\text{th}}}{\varphi\Omega_2}\right)^{\frac{\alpha_2}{2}}\right)^{\frac{2}{\alpha_2}}}{\varphi}\gamma_{\text{th}}\,\middle|\,\begin{matrix}\left(\frac{2}{\alpha_1}\left(\alpha_1(\mu_1+k)-\frac{\alpha_2}{2}m\right)+\frac{1}{1-\delta}+1,\frac{2}{\alpha_1}\right)\\ \left(0,\frac{2}{\alpha_2}\right),\left(\frac{2}{\alpha_1}\left(\alpha_1(\mu_1+k)-\frac{\alpha_2}{2}m\right),\frac{2}{\alpha_1}\right)\end{matrix}\right].\\
&\text{where } \delta = 1-\left(\left(\frac{2\mu_1 h_1}{\Omega_1{}^{\frac{\alpha_1}{2}}}\right)\left(\frac{\gamma_{\text{th}}}{\phi}\right)^{\frac{\alpha_1}{2}}\right)^{-1}
\end{aligned}
\tag{16}
$$

$$
\begin{aligned}
\text{OP} =& 1-\frac{\pi\alpha_1\mu_1^{2\mu_1}h_1^{\mu_1}}{\Gamma(\mu_1)\Omega_1{}^{\alpha_1\mu_1}\Gamma(\mu_2)\,2^{2\mu_2-1}\,h_2^{\mu_2}}\sum_{k=0}^{\infty}\sum_{l=0}^{\infty}\frac{1}{k!\Gamma(\mu_1+k+0.5)}\left(\frac{\mu_1 H_1}{\Omega_1{}^{\frac{\alpha_1}{2}}}\right)^{2k}\frac{1}{l!\Gamma(\mu_2+l+0.5)}\left(\frac{H_2}{2\,h_2}\right)^{2l}\\
&\times\frac{4}{\alpha_1\alpha_2}\frac{1}{\left(\frac{2\mu_1 h_1}{\Omega_1{}^{\frac{\alpha_1}{2}}}\right)^{\frac{2}{\alpha_1}\left(\alpha_1(\mu_1+k)-\frac{\alpha_2}{2}m\right)}}\mathrm{H}_{0,2}^{2,0}\left[\frac{\left(\frac{2\mu_1 h_1}{\Omega_1{}^{\frac{\alpha_1}{2}}}\right)^{\frac{2}{\alpha_1}}\left(2\mu_2\, h_2\left(\frac{\gamma_{\text{th}}}{\varphi\Omega_2}\right)^{\frac{\alpha_2}{2}}\right)^{\frac{2}{\alpha_2}}}{\varphi}\gamma_{\text{th}}\,\middle|\,\begin{matrix}---\\ \left(0,\frac{2}{\alpha_2}\right),\left(\frac{2}{\alpha_1}\left(\alpha_1(\mu_1+k)-\frac{\alpha_2}{2}m\right),\frac{2}{\alpha_1}\right)\end{matrix}\right]\\
&-\frac{\pi\alpha_1\mu_1^{2\mu_1}h_1^{\mu_1}}{\Gamma(\mu_1)\Omega_1{}^{\alpha_1\mu_1}\Gamma(\mu_2)\,2^{2\mu_2-1}\,h_2^{\mu_2}}\sum_{k=0}^{\infty}\sum_{l=0}^{\infty}\frac{1}{k!\Gamma(\mu_1+k+0.5)}\left(\frac{\mu_1 H_1}{\Omega_1{}^{\frac{\alpha_1}{2}}}\right)^{2k}\frac{1}{l!\Gamma(\mu_2+l+0.5)}\left(\frac{H_2}{2\,h_2}\right)^{2l}\\
&\times\frac{4}{\alpha_1\alpha_2}\frac{\Gamma\left(1+\frac{1}{1-\delta}\right)}{\left(\frac{2\mu_1 h_1}{\Omega_1{}^{\frac{\alpha_1}{2}}}(1-\delta)\right)^{\frac{2}{\alpha_1}\left(\alpha_1(\mu_1+k)-\frac{\alpha_2}{2}m\right)}}\mathrm{H}_{0,2}^{2,0}\left[\frac{\left(\frac{2\mu_1 h_1}{\Omega_1{}^{\frac{\alpha_1}{2}}}(1-\delta)\right)^{\frac{2}{\alpha_1}}\left(2\mu_2\, h_2\left(\frac{\gamma_{\text{th}}}{\varphi\Omega_2}\right)^{\frac{\alpha_2}{2}}\right)^{\frac{2}{\alpha_2}}}{\varphi}\gamma_{\text{th}}\,\middle|\,\begin{matrix}\left(\frac{2}{\alpha_1}\left(\alpha_1(\mu_1+k)-\frac{\alpha_2}{2}m\right)+\frac{1}{1-\delta}+1,\frac{2}{\alpha_1}\right)\\ \left(0,\frac{2}{\alpha_2}\right),\left(\frac{2}{\alpha_1}\left(\alpha_1(\mu_1+k)-\frac{\alpha_2}{2}m\right),\frac{2}{\alpha_1}\right)\end{matrix}\right].
\end{aligned}
\tag{17}
$$

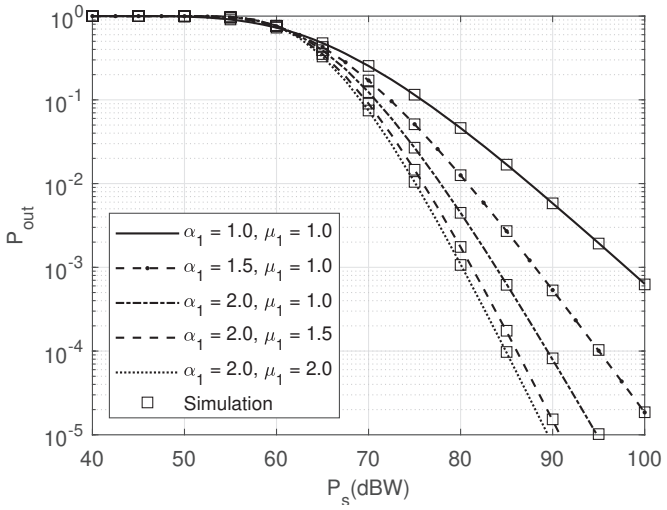

Fig. 1. OP as a function of P_s for the TSR protocol in α-η-μ with $\eta_1 = 0.5$ and d_1=20m, illustrating the effects of varying the S-R link fading parameters α_1 and μ_1.

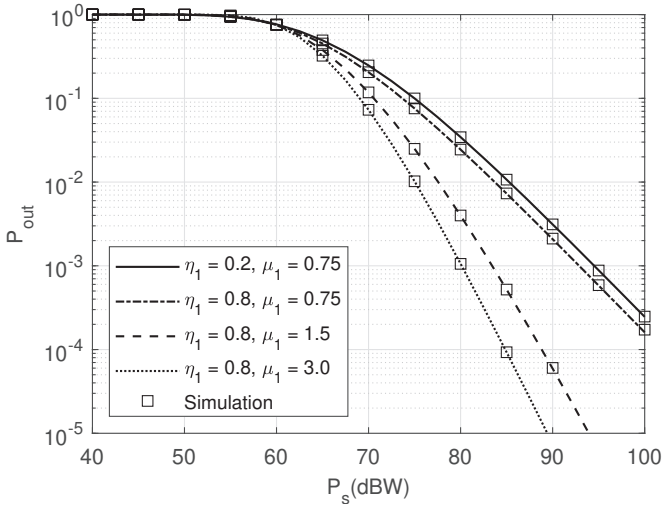

Fig. 2. OP versus P_s for the TSR protocol in α-η-μ fading channels, with $\alpha_1 = 1.5$ and d_1=20m, demonstrating the impact of varying the S-R link fading parameters η_1 and μ_1.

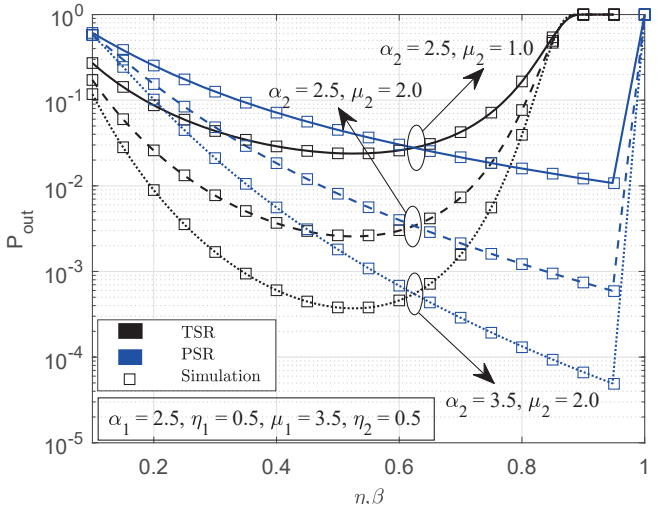

Fig. 3. OP as a function of η and β for TSR and PSR protocols in α-η-μ fading channels.

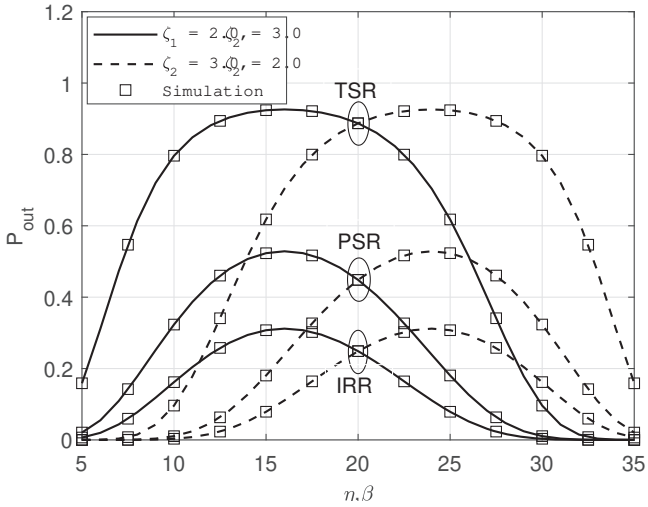

Fig. 4. OP as a function of d_1 along with path-loss exponents ζ_1 and ζ_2 for symmetrical channels $\alpha_1 = \alpha_2 = 3$, $\eta_1 = \eta_2 = 0.75$, and $\mu_1 = \mu_2 = 2$.

in *2016 IEEE Global Communications Conference (GLOBECOM)*. IEEE, 2016, pp. 1–7.

[10] I. Orikumhi, C. Y. Leow, and Z. Ding, "Wireless information and power transfer in mimo virtual full-duplex relaying system," *IEEE Transactions on Vehicular Technology*, vol. 66, no. 12, pp. 11 001–11 010, 2017.

[11] Y. Ye, Y. Li, D. Wang, and G. Lu, "Power splitting protocol design for the cooperative noma with swipt," in *2017 IEEE International Conference on Communications (ICC)*. IEEE, 2017, pp. 1–5.

[12] Y. Xu, C. Shen, Z. Ding, X. Sun, S. Yan, G. Zhu, and Z. Zhong, "Joint beamforming and power-splitting control in downlink cooperative swipt noma systems," *IEEE Transactions on Signal Processing*, vol. 65, no. 18, pp. 4874–4886, 2017.

[13] W. Han, J. Ge, and J. Men, "Performance analysis for noma energy harvesting relaying networks with transmit antenna selection and maximal-ratio combining over nakagami-m fading," *IET Communications*, vol. 10, no. 18, pp. 2687–2693, 2016.

[14] O. S. Badarneh and M. S. Aloqlah, "Performance analysis of digital communication systems over α-η-μ fading channels," *IEEE Transactions on Vehicular Technology*, vol. 65, no. 10, pp. 7972–7981, 2015.

[15] M. Abramowitz and I. A. Stegun, *Handbook of mathematical functions with formulas, graphs, and mathematical tables*. US Government printing office, 1968, vol. 55.

[16] I. S. Gradshteyn and I. M. Ryzhik, *Table of integrals, series, and products*. Academic press, 2014.

[17] I. Krikidis, S. Timotheou, S. Nikolaou, G. Zheng, D. W. K. Ng, and R. Schober, "Simultaneous wireless information and power transfer in modern communication systems," *IEEE Communications Magazine*, vol. 52, no. 11, pp. 104–110, 2014.

[18] D. Joseph and H. Haubold, "Extended reaction rate integral as solutions of some general differential equations," in *Proceedings of the Third UN/ESA/NASA Workshop on the International Heliophysical Year 2007 and Basic Space Science: National Astronomical Observatory of Japan*. Springer, 2010, pp. 41–51.